LEGIBILITY NOTICE

A major purpose of the Technical Information Center is to provide the broadest dissemination possible of information contained in DOE's Research and Development Reports to business, industry, the academic community, and federal, state and local governments.

Although a small portion of this report is not reproducible, it is being made available to expedite the availability of information on the research discussed herein.

1

Conf-830816--10

LA-UR--83-963

DE83 015240

Los Alamos National Laboratory is operated by the University of California for the United States Department of Energy under contract W-7405-ENG-36.

TITLE: FUEL MODELS AND RESULTS FROM THE TRAC-PF1/MIMAS TMI-2 ACCIDENT CALCULATION

AUTHOR(S): E. C. Schwegler
P. J. Maudlin

SUBMITTED TO: International Meeting on LWR Severe Accident Evaluation
Boston, MA 02107

FUEL MODELS AND RESULTS FROM THE TRAC-PF1/MIMAS TMI-2 ACCIDENT CALCULATION

E. C. Schwegler and P. J. Maudlin
Los Alamos National Laboratory
Los Alamos, New Mexico 87545

ABSTRACT

A brief description of several fuel models used in the TRAC-PF1/MIMAS analysis of the TMI-2 accident is presented, and some of the significant fuel-rod behavior results from this analysis are given. Peak fuel-rod temperatures, oxidation heat production, and embrittlement and failure behavior calculated for the TMI-2 accident are discussed. Other aspects of fuel behavior, such as cladding ballooning and fuel-cladding eutectic formation, were found not to significantly affect the accident progression.

INTRODUCTION

In analyzing phenomena occurring during light-water reactor (LWR) degraded-core accidents, accurate fuel behavior modeling is quite important because thermal energy from the fuel is one of the basic driving forces behind the coolant and fission-product behavior. This paper describes the most important fuel models considered in the TRAC-PF1/MIMAS analysis of the TMI-2 accident[1] and presents some significant fuel behavior results from that analysis.

DESCRIPTION OF FUEL MODELS

In this section, MIMAS code models for the following fuel-rod-related phenomena are briefly described: (1) fuel-rod temperature distribution, (2) cladding oxidation, hydrogen generation and steam starvation, and (3) cladding embrittlement and brittle failure criteria.

This analysis considered the reactor core to be divided into three radial rings and five axial levels. Within each cell defined by a radial and axial boundary, all fuel rod segments have the same average behavior and properties. Axial and radial conduction heat transfer between rod segments in different cells is not presently modeled in MIMAS.

The temperature field in the fuel rods is calculated by numerically solving the one-dimensional radial finite-difference approximation to the general conduction equation

$$\frac{1}{r}\left[\frac{\partial}{\partial r}\left(rk\ \frac{\partial T}{\partial r}\right)\right] + q''' = \rho C_p\ \frac{\partial T}{\partial t} \qquad (1)$$

The detailed form of the finite difference equations is given in Ref. 2. Under steady-state conditions, a fully implicit form of the finite difference equations is used, whereas for transient conditions, a semi-implicit form is utilized to assure compatability with the fluid-dynamics calculations. Pertinent materials properties correlations used in these equations are from Ref. 3, whereas the fuel decay heat behavior is from Ref. 4.

The zircalloy cladding oxide-layer growth rate dL/dt is assumed to follow parabolic kinetics, that is

$$dL/dt = (X_{H_2O})^2(A/L)\exp(-B/RT) \qquad (2)$$

where and B are empirical constants, R is the gas constant, and T is absolute temperature. Below 1760 K, the Cathcart correlation[5] is used for the values of A and B, while between 1760 K and the Zircalloy melting point, the Urbanic correlation[6] is used. The oxide-layer growth rate determines hydrogen production and oxidation energy release according to the equation

$$2H_2O + Zr = 2H_2 + ZrO_2 + 6.5\times10^6\ J/Kg\ Zr \qquad (3)$$

The quantity X_{H_2O} in Eq. 2 is the mole fraction of steam adjacent to the cladding. This term empirically accounts for steam starvation effects, because as more and more steam is consumed by the cladding oxidation, X_{H_2O} decreases thereby decreasing the oxidation rate given by Eq. 2.

The diffusion of oxygen into the unoxidized beta-phase Zircalloy results in cladding embrittlement, eventually to the point where the cladding will shatter under relatively modest thermal strains. In the MIMAS code, the Fick's law diffusion equation for oxygen in Zircalloy is solved for the cladding geometry using a scheme from Ref. 3. Sufficient oxygen is assumed liberated from the steam and (if fuel-cladding contact exists) from the fuel to maintain a saturated oxygen concentration at the cladding boundaries. The cladding is assumed to shatter when exposed to cooling rates of 100 K/s or greater if the cladding temperature exceeds 1700 K, if the oxygen concentration in the beta-

Zircalloy exceeds 90% of saturation, or if the oxygen concentration in the beta-Zircalloy exceeds 65 weight percent. The cladding is assumed to shatter when exposed to cooling rates as low as 5 K/s if less than 0.3 mm of cladding contains less than one weight percent oxygen.

ANALYSIS RESULTS

The cladding temperature histories for the five fuel-rod axial sections in the innermost core ring during the interval 9000 to 11880 s after the beginning of the TMI-2 accident are shown in Fig. 1. The exponential cladding temperature increases around 11000 s are caused by the initiation of rapid cladding oxidation above 1273 K. The extremely rapid cladding temperature increases in levels 3 to 5 are caused by the switch from Cathcart to Urbanic kinetics above 1760 K. The cladding temperature downturns that follow these exponential increases are caused by steam starvation, whereas the temperature perturbations that occur in the fuel-rod cladding around 10800 s are caused by control rod melting.

The rod linear heat rates caused by ZrO_2 formation as a function of time are shown in Fig. 2 for the innermost core ring. In this figure, axial level 5 decreases its oxidation rate as level 4 oxidation increases and contributes to steam starvation in level 5. This process proceeds down the rod length: level 3 oxidation contributes to steam starvation and oxidation power decrease in level 4, and level 2 does the same to level 3. Superimposed on this general pattern are fluctuations in the oxidation power production caused by self-starvation within a level and local temperature perturbations.

The MIMAS code predicts that, at the time the TMI-2 core was reflooded, the fuel-rod cladding in the upper 80% of the core was embrittled to the point where the thermal stresses induced by a 5 K/s cooling rate would cause rod breakup. Upon core reflood, a pulse of saturated steam caused almost immediate disintegration of the embrittled fuel sections. The exact times at which fuel rod disintegration was calculated to occur in the various core cells is shown in Table I. These times indicate that the breakup of the fuel in the core is rather incoherent in regard to location, but because the breakup occurs over a short time period, this incoherency is of little practical consequence.

Other interesting fuel behavior phenomena calculated by MIMAS to occur during the TMI-2 accident include extensive cladding ballooning, a small amount of fuel-cladding eutectic formation, and extensive control-rod melting with possible molten control-rod fuel-rod interaction. The analysis results indicate that the rod ballooning and limited eutectic formation had little effect on the overall accident progression. The large uncertainties that exist at present in molten control-rod modeling presents difficulty in estimating the magnitude of molten control-rod fuel-rod interaction that may have occurred in TMI-2.

SUMMARY

Steam starvation effects generally kept the fuel-rod temperatures below the Zircalloy melting point during the TMI-2 accident. Although extensive cladding ballooning was calculated for the upper part of the core, this did not significantly affect the overall TMI-2 accident progression. The disintegration of the upper 80% of the TMI-2 core during the reflood was spatially incoherent and was calculated to occur over a time period of approximately 36 s.

REFERENCES

1. P. J. Maudlin, et. al., "A Damage Assessment of TMI-2," Los Alamos National Laboratory report LA-UR-83-737 (1983).

2. "TRAC-PD2: An Advanced Best-Estimate Computer Program for Pressurized Water Reactor Loss-of-Coolant Accident Analysis," Los Alamos National Laboratory report LA-8709-MS (1981).

3. "MATPRO-Version 11 (Revision 1), A Handbook of Materials Properties for Use in the Analysis of Light Water Reactor Fuel Rod Behavior," NUREG/CR-0947, TREE-1280, Rev. 1 (1980).

4. T. R. England and W. B. Wilson, "TMI-2 Decay Power: LASL Fission-Product and Actinide Decay Power Calculations for the President's Commission on the Accident at Three Mile Island," LA-8041-MS (October 1979).

5. J. V. Cathcart, "Quarterly Progress Report on the Zirconium Metal-Water Oxidation Kinetics Program Sponsored by the NRC Division of Reactor Safety Research for October-December 1976," ORNL/NUREG/TM-87 (February 1977).

6. V. F. Urbanic and T. R. Heidrick, "High Temperature Oxidation of Zircalloy-2 and Zircalloy-4 in Steam," J. of Nuc. Mat. 75 (1978).

TABLE I

TIMES FOR FUEL-ROD DISINTEGRATION

Ring 1					
Axial Section	1	2	3	4	5
Disintegration Time after Reflood (s)	–	7.58	10.25	5.38	0.03
Ring 2					
Axial Section	1	2	3	4	5
Disintegration Time after Reflood (s)	–	22.80	10.25	36.15	0.03
Ring 3					
Axial Section	1	2	3	4	5
Disintegration Time after Reflood (s)	–	4.06	10.25	9.91	32.66

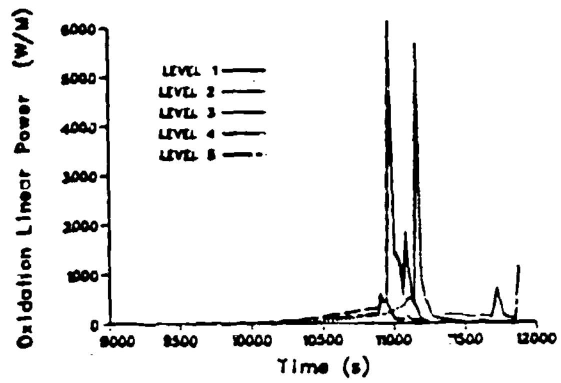

Fig. 2.
Cladding oxidation power vs time and axial position for core ring 1.

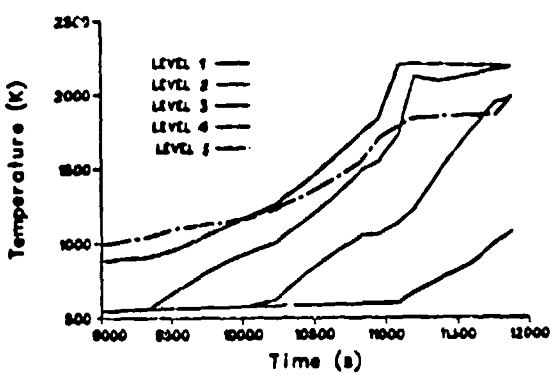

Fig. 1.
Cladding temperature vs time and axial position for core ring 1.